Regulation of Electrochemically Generated Ferrous Ions from an Iron Cathode for Pd-Catalytic Transformation of MTBE in Groundwater

ARTICLE *in* ENVIRONMENTAL SCIENCE & TECHNOLOGY · JUNE 2013

Impact Factor: 5.33 · DOI: 10.1021/es401730s · Source: PubMed

6 AUTHORS, INCLUDING:

Peng Liao
Chinese Academy of Sciences
31 PUBLICATIONS **320** CITATIONS
SEE PROFILE

Songhu Yuan
China University of Geosciences
67 PUBLICATIONS **1,157** CITATIONS
SEE PROFILE

Mingjie Chen
Sultan Qaboos University
36 PUBLICATIONS **172** CITATIONS
SEE PROFILE

Environmental Science & Technology

Article

pubs.acs.org/est

Regulation of Electrochemically Generated Ferrous Ions from an Iron Cathode for Pd-Catalytic Transformation of MTBE in Groundwater

Peng Liao,[†] Songhu Yuan,*[,†] Mingjie Chen,[‡] Man Tong,[†] Wenjing Xie,[†] and Peng Zhang[†]

[†]State Key Lab of Biogeology and Environmental Geology, China University of Geosciences, 388 Lumo Road, Wuhan 430074, P. R. China

[‡]Atmospheric, Earth and Energy Division, Lawrence Livermore National Laboratory, P.O. Box 808, L-184, Livermore, California 94550, United States

Supporting Information

ABSTRACT: A novel Pd-based electro-Fenton (E-Fenton) process has recently been developed to transform organic contaminants in groundwater. However, it only produces H_2O_2 and requires addition of Fe^{2+}. In this study, an innovative approach is developed to effectively regulate the generation of Fe^{2+} from an iron cathode in a three-electrode system in addition to H_2O_2 production. The Fe^{2+} is then used for the Pd-catalytic transformation of methyl *tert*-butyl ether (MTBE) in groundwater. Results from batch experiments suggest Fe^{2+} accumulation follows pseudo-first-order kinetics with rate quantitatively regulated by current and pH, and MTBE can be completely transformed. In a specially configured three-electrode column using iron as the first cathode, the localized acidic conditions develop automatically in the iron cathode and Pd zone by partitioning the current between the two cathodes, leading to controllable generation of Fe^{2+} and H_2O_2. Effects of electrolyte concentrations and types as well as humic acid on MTBE transformation are slight. The stable transformation (~70%) in a long-term study (20 days) suggests this improved Pd-based E-Fenton process is sustainable to produce Fe^{2+}, H_2O_2, and appropriate pH conditions simultaneously for transforming organic contaminants. This study presents a new concept of generating Fe^{2+} from an iron cathode for the processes requiring Fe^{2+}.

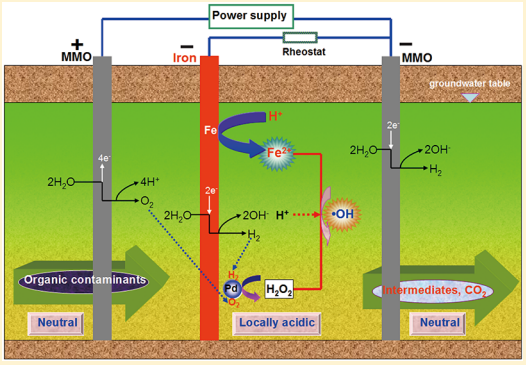

INTRODUCTION

Methyl *tert*-butyl ether (MTBE) has been manufactured almost exclusively for use as a fuel additive since the 1970s.[1−3] MTBE has been found in various environments, particularly in groundwater, because of its high solubility under ambient conditions (48 g/L).[1] For example, MTBE is frequently detected at gasoline spill sites with concentrations of tens or even hundreds of milligram per liter.[4,5] MTBE was reclassified by the USEPA as "carcinogenic in humans by all routes of exposure" based on findings that indicate side effects of headaches, vomiting, diarrhea, fever, cough, muscle aches, and skin and eye irritation.[1,6] Current processes that have been proposed for remediation of MTBE in groundwater include phase transfer,[7] in situ chemical oxidation (ISCO),[8] advanced oxidation technologies (AOTs),[9−11] and biodegradation.[2,12,13] Electrochemical processes have attracted increasing interests in groundwater remediation as they are simple and versatile.[14−17] Electro-Fenton (E-Fenton) processes, such as peroxi-coagulation (PC),[18] electrochemical peroxidation (ECP),[19] and anodic Fenton treatment (AFT),[20] are widely used in wastewater treatment.[21] However, in situ application of E-Fenton processes in groundwater remediation is limited by the requirements of O_2 for H_2O_2 production and appropriate pH conditions for contaminants oxidation because O_2 injection and pH adjustment are complicated and costly in the subsurface.

Recently, Yuan et al. developed a new Pd-based E-Fenton process,[14,15] which extends the application of E-Fenton processes from wastewater treatment to groundwater remediation. In this new process, H_2O_2 is produced in situ from the combination of electro-generated H_2 and O_2 on a Pd catalyst under acidic conditions (eqs 1−3). Automatic pH adjustments are achieved by appropriately arraying the electrodes.[15] This process has been shown to be highly effective in treating a wide range of recalcitrant contaminants (eqs 4 and 5).[14,15,22] It was found that the concentration of Fe(II) significantly affected the generation of hydroxyl radicals (•OH) from H_2O_2 (eq 4).[14,15,22] The intrinsic Fe(II) in aquifers was proposed to be the source of Fe(II),[14,15] which indicates an inefficiency in treating the iron-defective groundwater. A low concentration of Fe(II) is not sufficient for •OH generation,[14] while a high concentration competes with contaminants for •OH (eq 6). When Fe(II) is supplied to the iron-defective subsurface, Fe^{2+} is difficult to be tuned to an appropriate concentration because transport and fate of Fe(II) highly depends on groundwater pH and redox conditions.

Received: March 25, 2013
Revised: June 12, 2013
Accepted: June 16, 2013
Published: June 17, 2013

dx.doi.org/10.1021/es401730s | Environ. Sci. Technol. 2013, 47, 7918−7926

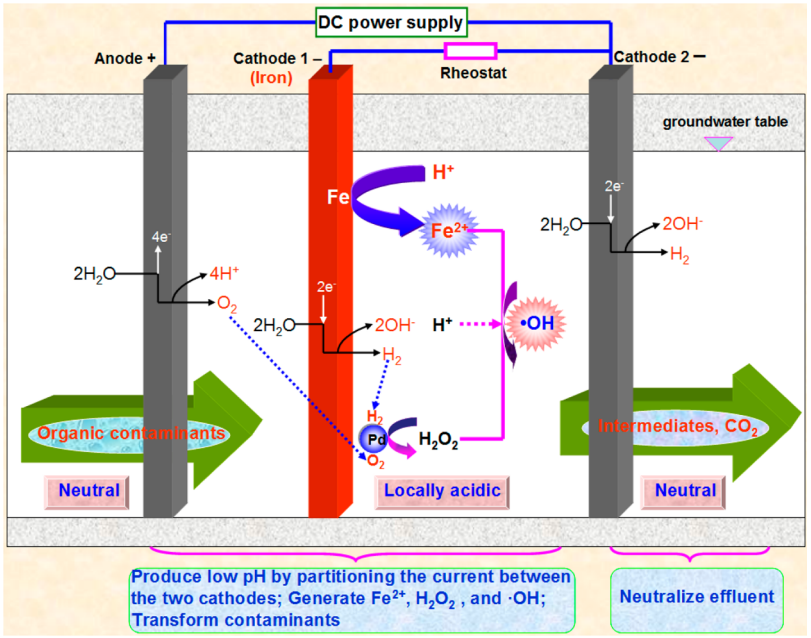

Figure 1. Conceptual model of regulation of electrochemically generated Fe^{2+} from an iron cathode for Pd-catalytic transformation of MTBE in groundwater.

$$2H_2O \rightarrow O_2 + 4H^+ + 4e^- \quad (1)$$

$$2H_2O + 2e^- \rightarrow H_2 + 2OH^- \quad (2)$$

$$H_2 + O_2 \xrightarrow{Pd} H_2O_2 \quad (3)$$

$$H_2O_2 + Fe^{2+} + H^+ \rightarrow Fe^{3+} + \bullet OH + H_2O \quad (4)$$

$$Orgs + \bullet OH \rightarrow Oxidation\ products \quad (5)$$

$$Fe^{2+} + \bullet OH \rightarrow Fe^{3+} + OH^- \quad k = 3.2 \times 10^8\ M^{-1}\ s^{-1}\ [21] \quad (6)$$

In Fenton-based processes, Fe(II) is normally supplied by the addition of ferrous salts,[23,24] sacrificed iron anode,[20,25] and iron-containing materials.[26,27] The addition of ferrous salts complicates the implementation process. Sacrificial iron anodes can be effective (eq 7) but produce a lot of iron sludge.[20,25] When iron is used as the anode, it corrodes preferentially and no O_2 is produced.[16] Therefore, there will be a lack of O_2 for H_2O_2 production as O_2 is a necessary reactant.[14] Although iron-containing materials, such as Fe_3O_4 and zero-valency iron (ZVI), can be mixed with Pd to supply Fe(II),[27−29] the reaction will deplete the materials, and precipitates on the Pd surface will decrease the catalytic activity and clog the aquifer.[30−32] It is also attempted to load iron oxides onto a porous cathode for Fe(II) supply, but the concentration of Fe(II) reached as high as 24.4 mM within 120 min under neutral conditions,[33] suggesting a quick dissolution of the cathode. It is currently difficult or even impractical to fabricate large dimensions of stable porous cathodes for in situ groundwater remediation. Therefore, it is crucial to seek a new cost-effective strategy to supply Fe(II) for the Pd-based E-Fenton process.

$$Fe - 2e^- \rightarrow Fe^{2+} \quad (7)$$

$$Fe + 2H^+ \rightarrow Fe^{2+} + H_2 \quad (8)$$

In this study, a new concept of in situ generating Fe^{2+} from an iron cathode is proposed for the Pd-based E-Fenton process. The conceptual model of this improved Pd-based E-Fenton process is presented in Figure 1. One anode and two cathodes are arrayed to sustain water electrolysis, thus supplying H_2 and O_2 for H_2O_2 production on the Pd surface (eqs 1−3).[15,22] The localized acidic conditions in cathode 1 and Pd zone automatically develops as there are more H^+ ions produced at the anode than OH^- ions produced at the adjacent cathode (cathode 1). Neutral effluent is attained when groundwater passes through cathode 2. Iron is employed as the first cathode. Under the localized acidic conditions, the iron cathode acts as a source of Fe^{2+} release by chemical corrosion (eq 8)[34] in addition to H_2 and OH^- production by water electrolysis. Natural corrosion of iron under acidic conditions (~pH 3) produces more than enough Fe^{2+} for H_2O_2 decomposition (eq 4). Interestingly, a negative applied current applied on the iron cathode can inhibit the corrosion by cathodic protection effect.[35−37] Theoretically, the extent of inhibition can be regulated by adjusting the cathodic current. In this improved Pd-based E-Fenton process, no chemicals will be added during the course of remediation because all the reactants (Fe^{2+} and H_2O_2) and conditions (~pH 3) can be automatically produced. Moreover, the concentrations of Fe^{2+} and H_2O_2, as well as pH conditions, can be manually regulated by adjusting the total current and the current partition. As cathodic protection is always recognized as an effective means of anticorrosion, the concept of generating Fe^{2+} from the iron cathode represents an alternative to the conventional means of Fe^{2+} production, i.e., by iron anode and zerovalent iron.

Using MTBE as a representative of groundwater contaminants, the performance of the aforementioned improved Pd-based E-Fenton process is tested for Fe(II) generation and MTBE transformation. For the sake of simplicity, an undivided electrolytic cell with an iron cathode is first used to model the kinetics of Fe^{2+} accumulation at different values of pH and current. Pd-catalytic transformation of MTBE is also examined. Then, the conceptual model of the improved Pd-based E-Fenton process is justified in a specially configured three-

dx.doi.org/10.1021/es401730s | Environ. Sci. Technol. 2013, 47, 7918−7926

electrode column using an iron cathode. Fe^{2+} accumulation in the iron cathode and Pd zone is electrochemically regulated by varying the cathodic current applied on the iron cathode. MTBE transformation at different times along the column is described. The effects of groundwater compositions on MTBE transformation are examined. The long-term performance of this column is ultimately evaluated.

EXPERIMENTAL SECTION

Chemicals. MTBE (99.8%), *tert*-butyl alcohol (TBA, 99.5%), and humic acid sodium salt (HA, 99.5%) were purchased from Sigma-Aldrich. *tert*-Butyl formate (TBF, 99.5%), acetone (AC, 99.5%), formaldehyde (FA, 37%), and formic acid (99.5%) were supplied by Aladdin Chemistry Co. Ltd. Palladium on alumina powder (5% wt. Pd, Shanxi Kaida Chemical Ltd.), with a particle size of 1.5 to 5 μm, was used as the catalyst in the batch experiments. Palladium on alumina pellets (0.5% wt. Pd, Shanxi Kaida Chemical Ltd.) 2.5 to 3.5 mm in size was used in the column experiments. Iron plate (S45C type, Wuhan Steel Processing Co., Ltd.) and mixed metal oxides (MMO, IrO_2 and Ta_2O_5 coating on titanium diamond mesh, Shanxi Kaida Chemical Ltd.) with dimensions of 5.0 cm diameter and 1.7 mm thickness were used as the electrodes. Seventeen holes (4.1 mm in diameter) were evenly distributed through the iron plate electrodes. Prior to the experiments, the iron electrode was polished with coarse emery cloth, etched by diluted HCl solution (5 wt %), and washed with deionized water. Deionized water (18.2 mΩ·cm) obtained from a Millipore Milli-Q system was used in all the experiments. All the chemicals used in this study were above analytical grade.

Batch Experiments. An undivided acrylic electrolytic cell was used to evaluate Fe^{2+} generation for MTBE transformation at ambient temperatures (25 ± 1 °C) (Figure S1 in the Supporting Information). An MMO mesh and an iron plate were respectively used as the anode and cathode, with 40 mm spacing in parallel positions. For each test, 400 mL of 20 mg/L MTBE solution was transferred into the cell, and 10 mM Na_2SO_4 and 1 g/L Pd/Al_2O_3 (5% wt. Pd) were attained by the addition of specific masses of Na_2SO_4 and Pd/Al_2O_3 powder. Na_2SO_4 was used as the background electrolyte because it commonly exists in groundwater and exerts negligible influence on mechanism analysis.[14] Moreover, our previous study revealed that anionic electrolytes (SO_4^{2-}, Cl^-, HCO_3^- and NO_3^-) in the concentration level less than 10 mM had slight influence on TCE transformation.[14] Aqueous pH was adjusted manually to 3.0 by the dropwise addition of 1 M H_2SO_4. For comparison, an MMO mesh was used as the cathode in the presence of 10 mg/L Fe^{2+}. The reactor was immediately sealed and stirred at 600 rpm using a Teflon-coated magnetic stirring bar. A constant electric current of 50 mA (2 mA/cm^2) was applied with a cell potential of about 4 V. The electrode potentials for the iron cathode and the MMO anode were −2.1 and 1.1 V (versus SCE), respectively. The aqueous solution was sampled at predetermined time intervals for analysis of MTBE and its transformation products, iron species, pH, H_2O_2, and •OH concentration. All experiments were carried out in duplicate.

Column Experiments. From the viewpoint of practical application, a vertical acrylic tube column (5.0 cm inner diameter × 30 cm length) was used to validate the aforementioned conceptual model of the improved Pd-based E-Fenton process (Figure S2). Three electrodes were mounted in the upward sequence of anode (MMO), cathode 1 (iron plate), and cathode 2 (MMO). 4.5 g of Pd/Al_2O_3 pellets were supported by cathode 1 (iron plate) to produce a pellet bed monolayer. The remaining space in the column was packed with 4 mm glass beads with a porosity of 0.46. The total and pore volume (PV) were 588 and 268 mL, respectively. Solution was pumped through the bottom of the columns at a rate of 2.5 mL/min using a peristaltic pump (Luxi, model HL-2, China). The flow rate was maintained at 2.5 mL/min, resulting in Darcy's velocity of 1.83 m/day. The total current was kept at 80 mA by a DC power supply (GPC-3060D, Taiwan Goodwill Instrument). By adjusting the rheostat, different currents were partitioned between cathodes 1 (iron plate) and 2 so that the localized pH in the iron cathode and Pd zone could be regulated automatically without acid or base addition.

Simulated MTBE-contaminated groundwater (10 mg/L) was prepared in three sets of electrolyte deoxygenated solution and was stored in a 5 L gastight collapsible bag. The first set of groundwater (GW-1) contained 5 mM Na_2SO_4 and 0.5 mM $CaSO_4$ with the conductivity of ∼1240 μS/cm. The second set of groundwater (GW-2) with a relatively low conductively (∼600 μS/cm) was synthesized according to the composition of groundwater in an MTBE-contaminated site in the US.[38] The third set of groundwater (GW-3) was sampled from the shallow aquifer in Wuhan city, China (114°24′ E, 30°33″ N) with the conductively of ∼550 μS/cm. The city shallow groundwater is tested because it often suffers from MTBE contamination resulting from numerous gas stations. The compositions of GW-2 and GW-3 are listed in Table S1. The column was flushed by 2 PVs of contaminated groundwater before switching on the power supply. Control experiments show that the adsorption of MTBE on Pd/Al_2O_3 pellets and glass beads were negligible during operation. At predetermined time intervals, about 1 mL of groundwater was taken out from six ports (see Figure S2 for locations) and measured for MTBE, pH, and iron species concentration.

Chemical Analysis. MTBE, TBF, TBA, and AC concentrations were analyzed using a gas chromatograph (GC, Shimadzu 2014C, Japan) equipped with a flame ionization detector (FID), a capillary column (30 m × 0.32 mm ×0.5 μm), and a headspace concentrator (DK-3001A, Beijing Zhongxing Huili Technology Development Co., Ltd.). The column temperature was held at 35 °C for 2 min, heated from 35 to 60 °C at a rate of 5 °C/min, and then cooled to 35 °C at a rate of 10 °C/min. The injector and detector temperatures were set at 220 and 250 °C, respectively. Two mL of the aqueous sample was collected and injected into a 20-mL headspace vial sealed with septa. The equilibrium temperature in the vial was set to 105 °C. The detection limits for all compounds were 0.1 mg/L. Gas concentrations were calculated by Henry's law. FA was analyzed by an LC-15C HPLC (Shimadzu) equipped with a UV detector and an XDB-C18 column (4.6 × 50 mm) after derivatization with 2,4-dinitrophenylhydrazine.[39] The mobile phase used a mixture of acetonitrile and water (60:40, v/v) at 1 mL/min, with the detection wavelength at 355 nm. Carboxylic acids were also measured by HPLC. The mobile phase used a mixture of phosphoric buffer (pH 2.7) and methanol at 99:1 (v:v) at 0.8 mL/min and a detection wavelength of 210 nm. The detection limits for FA and carboxylic acids were 1 μM.

H_2O_2 concentration was determined at 405 nm by a spectrometer (UV-1800 PC, Shanghai Mapada Spectrum Instrument Co., Ltd.) after coloration with $TiSO_4$.[40] The

•OH levels were determined using dimethyl sulfoxide (DMSO) trapping and HPLC methods described in previous literature.[41] Iron species were measured at 510 nm using the 1,10-o-phenanthroline analytical method.[42] The corrosion potentials of the iron electrode at various pH and at 50 mA were measured on a CS150 electrochemical workstation (Wuhan CorrTest Instrument, China) using a Pt electrode as the counter electrode and a saturated calomel electrode (SCE) as the reference electrode. The electrolyte used for measurement was 10 mM $NaSO_4$.

RESULTS AND DISCUSSION

Generation of Fe^{2+} from Iron Cathode for MTBE Transformation. For the sake of simplicity, an undivided electrolytic cell with an iron cathode was first used to investigate the mechanism and kinetics of Fe^{2+} accumulation and MTBE transformation under different conditions. Figure 2a shows the variation in the MTBE concentration under conditions of pH 3, 50 mA current, and 1 g/L Pd/Al_2O_3. The control experiment using the iron cathode without an applied current or Pd catalyst does not present any significant transformation of MTBE. In the presence of Pd/Al_2O_3, MTBE (20 mg/L) was completely transformed in 60 min following pseudo-first-order kinetics with a rate constant of 0.040 min^{-1}. For comparison, the experiment was also conducted using an MMO cathode in the presence of 10 mg/L Fe^{2+}, which is the average concentration accumulated in the cell using the iron cathode. This showed a slower MTBE transformation with a pseudo-first-order rate constant of 0.036 min^{-1}. The rate constant of MTBE transformation normalized by Pd concentration (0.05 g_{Pd}/L) using the iron and MMO cathode is 0.80 and 0.72 L g_{Pd}^{-1} min^{-1}, respectively, which is in the same level as that reported by Munakata and Reinhard [43] and 1 order of magnitude smaller than that reported by Lowry and Reinhard[44] using Pd and H_2 for TCE hydrodechlorination.

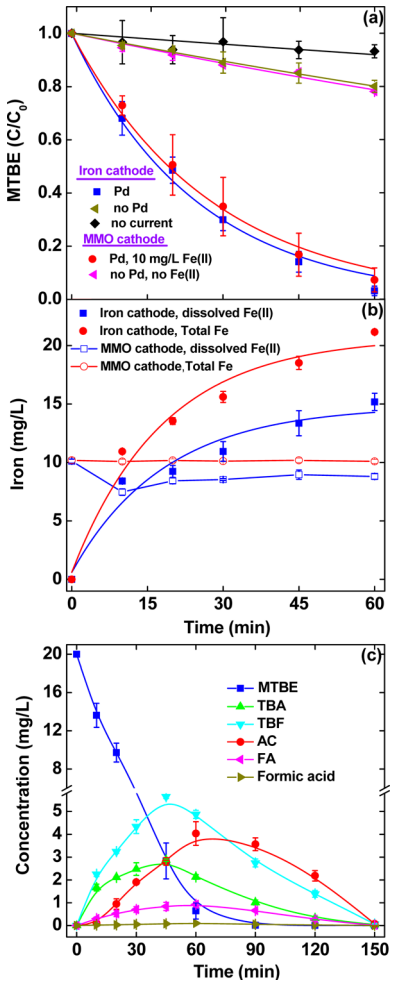

Figure 2. (a) Transformation of MTBE and (b) variations of iron species concentration in the electrolytic cell and (c) profiles of MTBE transformation using the iron cathode. The reaction conditions using the iron cathode are based on 20 mg/L initial MTBE concentration, pH 3.0, 1 g/L Pd/Al_2O_3, and 10 mM Na_2SO_4 background electrolyte. The reaction conditions using the MMO cathode are the same as those using the iron cathode except that 10 mg/L Fe^{2+} was added. Curves refer to pseudo-first-order kinetic fittings. Error bars indicate 95% confidence intervals.

The efficient transformation of MTBE proves that it is feasible to generate Fe^{2+} ions from an iron cathode for Pd-catalytic transformation of organic contaminants in groundwater. The concentration of Fe^{2+} increases to a plateau at about 14 mg/L within 60 min of using the iron cathode and decreases from the initial 10 mg/L to 8 mg/L using the MMO cathode (Figure 2b). The solution pH increased from 3.0 to 3.3 using the iron cathode. A parallel test using the MMO cathode had minimal variation of the pH. The pH increase is attributed to the consumption of H^+ ions by chemical corrosion of the iron cathode (eq 8). The concentration of Fe^{2+} released from chemical corrosion due to a rise in the pH was calculated to be 14 mg/L within 60 min, which is in good agreement with the measured cumulative concentration. In addition, the corrosion potential (Eh) of the iron electrode under conditions of pH 3 was measured to be −0.440 V (Figure S3a), falling in the corrosion region (Figure S3b). As a result, chemical corrosion of the iron cathode is responsible for Fe^{2+} generation under the protection of cathodic current.

H_2O_2 produced from the combination of H_2 and O_2 on Pd surface (eqs 1−3) is responsible for contaminant transformation.[14,15,22] The cumulative H_2O_2 concentration reaches approximately 14 mg/L within 60 min in the presence of Pd/Al_2O_3 and absence of Fe^{2+} (Figure S4). H_2O_2 can be decomposed to powerful oxidizing radicals of •OH (oxidation potential: 2.8 V/SHE) in the presence of Fe^{2+} (eq 4). The cumulative concentration of •OH radicals increases for both systems using the iron and MMO cathodes (Figure S5). Good correlation between MTBE transformation rate constants and •OH generation rate constants (Figure S6) indicates that •OH was mainly responsible for MTBE transformation ($k_{MTBE-•OH}$ = 1.6×10^9 M^{-1} s^{-1} [1]). The ratio of H_2O_2 to Fe^{2+} is critical for the transformation efficiency.[24,45] H_2O_2 and Fe^{2+} were generated gradually using the iron cathode. In the cell using the MMO cathode, Fe^{2+} concentration was in excess relative to the H_2O_2 concentration during the first stage but was defective in the later stage. In this regard, using an iron cathode is advantageous over the external addition of Fe(II) in terms of Fe^{2+} supply.

The primary transformation intermediates of MTBE using the iron cathode included TBF, AC, TBA, FA, and formic acid (Figure 2c). All these intermediates accumulated gradually with the disappearance of MTBE in the initial 60 min and disappeared afterward by prolonging the treatment time. This suggests a high oxidation ability of this system. Other intermediates reported for MTBE oxidation such as methyl acetate, 2-methoxy-2-methyl propionaldehyde, pyruvaldehyde,

dx.doi.org/10.1021/es401730s | Environ. Sci. Technol. 2013, 47, 7918−7926

hydroxyacetone, pyruvic acid, acetic acid, and oxalic acid were not detected in this study.[1,3,6,9] Accumulation of intermediates is due to their low reaction rates with •OH, which are 1 or 2 orders of magnitude lower than that of MTBE.[46] The intermediates identified in this study are similar to those reported in MTBE oxidation by anodic Fenton[47] and UV/H_2O_2.[10]

Mechanism and Kinetics of Fe^{2+} Accumulation. When electricity is applied to the iron cathode, accumulation of Fe^{2+} depends on the current and solution pH. The decreasing solution pH increases the rate of chemical corrosion of the iron cathode (eq 8).[34] The increasing current increases the electron density on the iron cathode, which suppresses the release of electrons from the iron corrosion (reverse reaction of eq 7).[35,48] The accumulation of Fe^{2+} also decreases at high pH due to precipitation and oxidation (eq 9).[49] Regeneration of Fe^{2+} by iron cathode is difficult because Fe^{2+} is continuously released from the corrosion of iron cathode under acidic conditions, and consumption of Fe^{2+} by H_2O_2 is neglected because the experiments for analysis of Fe^{2+} accumulation kinetics were conducted in the absence of Pd/Al_2O_3. Therefore, the rate of Fe^{2+} accumulation using an iron cathode in the absence of Pd/Al_2O_3 is derived as eq 10 (see details in Section S1)

$$4Fe^{2+} + 8OH^- + O_2 + 2H_2O \rightarrow 4Fe(OH)_3(s)$$
$$pK_{sp} = 38.55 \quad (9)$$

$$\frac{d[Fe(II)]}{dt} = k_H^+ \bullet [H^+]^2 \bullet [Fe] - k_e^- \bullet [n_{e-}]^2 \bullet [Fe^{2+}] - k_{OH}^- \bullet [OH^-]^2 \bullet P_{O2} \bullet [Fe^{2+}]$$
$$= k \bullet [Fe^{2+}] \quad (10)$$

where k ($=k_H^{+\prime} \bullet 10^{-2pH} - k_e^- \bullet k' \bullet I^2 - k_{OH}^- \bullet P_{O2} \bullet 10^{2pH-28}$) is the apparent accumulation rate constant of Fe^{2+}, and k_H^+, k_e^-, and k_{OH}^- are the rate constants for Fe^{2+} generation by H^+ (eq 8), inhibition of Fe^{2+} generation by cathode electrons (reverse reaction of eq 7), and Fe^{2+} consumption by OH^- and O_2 (eq 9), respectively. $[n_{e-}]$ is the electron density concentration, and P_{O2} is the partial pressure of oxygen. $k_H^{+\prime}$ and k' are constants. Therefore, the accumulation of Fe^{2+} conforms to pseudo-first-order kinetics, and the rate constant can be quantitatively regulated by electric current and solution pH.

Figure 3 displays the dependence of Fe^{2+} accumulation at different currents and pHs using the iron cathode. At pH 3, the accumulation of Fe^{2+} at different currents approximately follows pseudo-first-order kinetics. The rate constant of Fe^{2+} accumulation decreases from 0.049 min^{-1} without an applied current to 0.003 min^{-1} at 80 mA (inset in Figure 3a). When the current is higher than 120 mA, Fe^{2+} accumulation is minimal because of the low k values (close to zero). At 50 mA, the accumulation of Fe^{2+} at different pHs also follows pseudo-first-order kinetics (Figure 3b). The rate constant of Fe^{2+} accumulation decreases from 0.021 to 0.0001 min^{-1} as the solution pH increases from 2 to 7 (inset in Figure 3b), which is due to the greater inhibition of iron cathode corrosion at higher pH at a specific current (Figure S3).[34] Similar results were found at currents of 0, 20, and 80 mA (Figure S8). When the solution pH was elevated to 5, Fe^{2+} did not accumulate significantly, which is consistent with the fact that minimal Fe^{2+} accumulates at pH 7 at any applied current (Figure S8). The

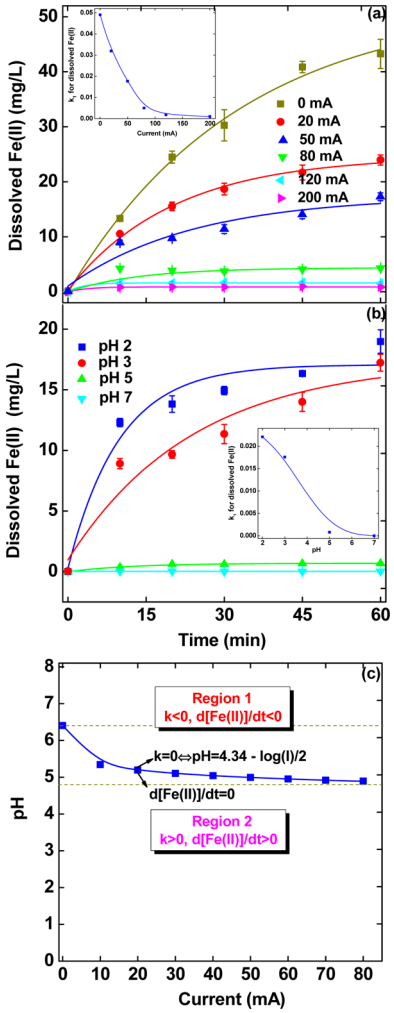

Figure 3. Effect of (a) current and (b) pH on accumulation of Fe^{2+} using the iron cathode and (c) relationship of current and pH for accumulation of Fe^{2+}. Unless otherwise specified, the reaction conditions are based on pH 3, 50 mA current, and 10 mM Na_2SO_4 background electrolyte. Curves refer to pseudo-first-order kinetic fittings. The insets in (a) and (b) illustrate the pseudo-first-order rate constants of Fe^{2+} accumulation versus current and pH, respectively. Error bars indicate 95% confidence intervals.

relatively high correlation coefficients ($R^2 > 0.919$) suggest that the kinetic model (eq 10) is reasonable for Fe^{2+} accumulation.

To further reveal the relation of Fe^{2+} accumulation with current and pH, Figure 3c depicts the contour map of Fe^{2+} accumulation at different currents and pHs. When k is set at zero in eq 10, the values of $k_H^{+\prime}$, k_e^-, and k_{OH}^- were calculated to be 4.8×10^4 M^{-2} s^{-1}, 8.9×10^9 M^{-2} s^{-1}, and 1.4×10^{12} M^{-2} Pa^{-1} s^{-1} at pH 2 without electricity application, at pH 3 and 50 mA current, and at pH 5 and 50 mA current, respectively.[50] A positive value of k suggests that Fe^{2+} accumulates, while a negative value of k indicates that Fe^{2+} cannot accumulate. Consequently, Fe^{2+} accumulates when the pH value is below the curve (region 2) and cannot accumulate when the pH value is above the curve (region 1).

Electrochemically Regulated Fe^{2+} Generation in a Three-Electrode Column. For this study, a three-electrode column using an iron cathode (Figure S2) was specially configured to regulate the localized pH in the iron cathode and Pd zone for generation of Fe^{2+} and H_2O_2 by adjusting the

dx.doi.org/10.1021/es401730s | Environ. Sci. Technol. 2013, 47, 7918−7926

current partition between cathodes 1 (iron cathode) and 2. When the current applied on the iron cathode increased from 30 to 50 mA, the pH in the vicinity of iron cathode increased slightly from 3.0 to 3.5 (Figure 4a). With the current further raised to 80 mA, the localized pH remarkably increases to 8. It is noted that the stabilized pH of the effluent declined from 11.5 to 7.5 when the current applied on the iron cathode increased from 30 to 80 mA (Figure 4a). An exponential relationship (eq 11) between the pH and current is observed in the iron cathode zone (inset in Figure 4a). This monotone function indicates that the localized pH is determined by the current applied on the iron cathode, which differs from the batch experiments where the pH is adjusted manually.

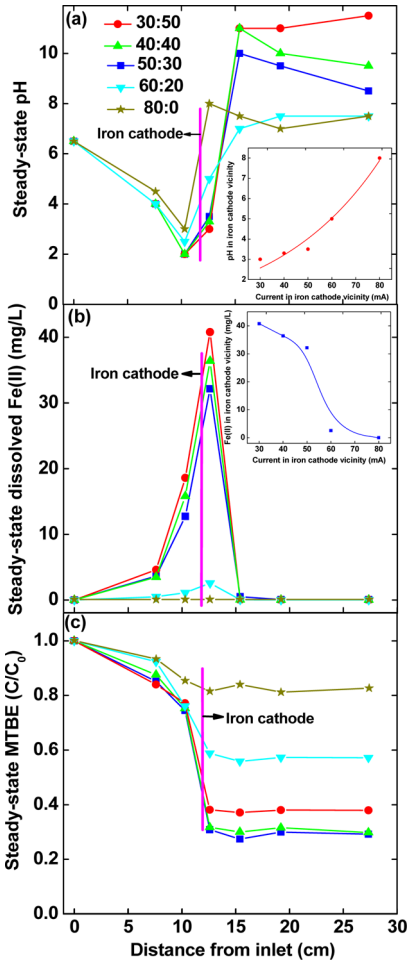

Figure 4. Effect of current partition on the steady-state variations of (a) pH, (b) dissolved Fe^{2+} concentration, and (c) MTBE along the column. The inset in (a) illustrates the linear regression between pH and current in the vicinity of iron cathode. The inset in (b) denotes the linear regression between Fe^{2+} concentration and current in the vicinity of iron cathode. Operation conditions are based on 10 mg/L initial MTBE concentration, 5 mM Na_2SO_4 and 0.5 mM $CaSO_4$ electrolyte, 2.5 mL/min, and a total current of 80 mA with different partitions in cathodes 1 and 2.

$$\mathrm{pH} = 1.3 \bullet \exp(I_{\mathrm{iron}}) \ (30 \le I \le 80\ \mathrm{mA}) \quad R^2 = 0.973 \tag{11}$$

As the localized pH is determined by the current on the iron cathode, accumulation of Fe^{2+} can be exclusively regulated by the current. Figure 4b shows that the steady-state Fe^{2+} concentration along the column decreases from maximum values in the iron cathode zone to the low values in both sides of the iron cathode. It should be noted that the regeneration of Fe^{2+} on the cathode 2 is minimal because Fe^{2+} is quickly transformed to Fe(III)-precipitates under the oxic and neutral or alkaline conditions.[15,21] Cumulative Fe^{2+} concentrations in the vicinity of the iron cathode at different current partitions follow the order of 30:50 > 40:40 > 50:30 > 60:20 > 80:0. This was confirmed by a slight decrement as the current on the iron cathode increased from 30 to 50 mA (inset in Figure 4b), followed by a dramatic decrease to a low value below the detection limit as the current increased to 80 mA. Decreasing the current on the iron cathode speeds up Fe^{2+} generation. However, excess Fe^{2+} may consume H_2O_2 and quench $^{\bullet}OH$ (eq 6),[14,15,21−24] and a low current on the iron cathode can lead to an alkaline effluent. It is therefore important to tune the current on the iron cathode to an appropriate level for generating the required concentration of Fe^{2+} ions.

MTBE Transformation in the Column. In the three-electrode column using an iron cathode, MTBE (10 mg/L) transformation attains steady state after 150 min of operation (1.4 PVs) in a typical column (Figure S9). As shown in Figure 4c, MTBE can be efficiently transformed in the Pd zone. The primary transformation intermediates are similar to those in the two-electrode system (Figure S10). Transformation of MTBE and intermediates on cathode 2 was negligible because oxidizing species cannot be generated under alkaline conditions.[15,21] With the five ratios of current partition, the removal rates of MTBE are in the sequence 50:30 > 40:40 > 30:50 > 60:20 > 80:0, implying the critical role of current partition on MTBE transformation. The anodic current generates O_2 and H^+ (eq 1), and the cathodic current partitioned on the iron (first cathode) generates H_2 and OH^- (eq 2). As the quantity of H^+ produced at the anode is more than that of OH^- produced at iron (first cathode), and the reflux of OH^- from cathode 2 is complex, a low pH in local Pd zone was automatically developed, which contributes to the production of Fe^{2+} (eq 8), H_2O_2 (eq 3), and $^{\bullet}OH$ (eq 4). The lowest transformation of MTBE at the current ratio of 80:0 is likely due to the minimal generation of $^{\bullet}OH$ from Fe^{2+} and H_2O_2 under alkaline conditions (pH 8).[21] The low efficiency of transformation at the current ratio of 60:20 is a result of the low concentrations of Fe^{2+} and H_2O_2 at pH 5.[22] At the current ratio of 30:50, the higher Fe^{2+} concentration generated competes with MTBE for $^{\bullet}OH$.[21,23,24] Although similar efficiencies were obtained for current ratios of 50:30 and 40:40, the effluent is alkaline (Figure 4a) and the energy consumption is higher for the latter ratio (Table S2). Although partial current is partitioned in cathode 2 for pH regulation, the three-electrode system (30:50) is still more energy-saving in terms of transforming MTBE than the conventional two-electrode system (Table S2). In comparison with our previous results,[15,22] the improved three-electrode column is able to generate Fe^{2+} and H_2O_2 simultaneously without chemical addition.

To further evaluate the applicability of this process for real groundwater remediation, the effects of groundwater chemistry are investigated. Results show that transformation of MTBE (Figure 5) and generation of Fe^{2+} (Figure S11b) in GWs 2 and 3 were comparable to those in GW 1. This indicates that commonly existing electrolytes in actual groundwater, including SO_4^{2-}, Cl^-, NO_3^-, HCO_3^-, Na^+, K^+, Ca^{2+}, and Mg^{2+} (Table S1), did not cause any significant influence on the transformation

dx.doi.org/10.1021/es401730s | Environ. Sci. Technol. 2013, 47, 7918−7926

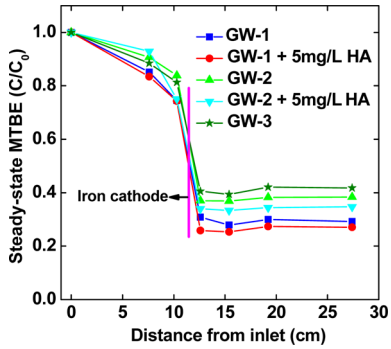

Figure 5. Effect of groundwater compositions on the steady-state variations of MTBE along the column. Operation conditions are based on 10 mg/L initial MTBE concentration, 2.5 mL/min, and a total current of 80 mA with 50 and 30 mA partitioned in cathodes 1 and 2. The compositions of GW-1 are 5 mM Na_2SO_4 and 0.5 mM $CaSO_4$. The compositions of GW-2 and GW-3 are listed in Table S1.

efficiency at less than 2 mM. The presence of 2 mM bicarbonate in groundwater has negligible impact on pH regulation (Figure S11a). The inhibitory effect of Cl^- on $^{\bullet}OH$-induced oxidation is not observed because it occurs in the presence of high concentration (20 mM).[14,51] It is worth noting that the presence of 5 mg/L HA facilitated MTBE transformation. This is probably because HA can act as an electron shuttle enhancing the production of $^{\bullet}OH$.[52] As a consequence, it can be suggested that the improved three-electrode column has the potential of application in a certain range of groundwater compositions.

Long-Term Performance for MTBE Transformation. The long-term MTBE transformation performance of the three-electrode column using an iron cathode is also evaluated. Figure 6a shows that MTBE transformation can be sustained at a stable level of around 70% for 20 days. About 30−40% MTBE is transformed in the anodic zone (Ports 1 and 2), which may be caused by the fact that certain Fe^{2+} and H_2O_2 produced in the iron cathode zone diffuses into the anode zone under the localized acidic condition. This finding suggests that the reaction zone was extended by convection-dispersion effects. The localized pH in the iron cathode zone decreases from 6.5 to 3.5 in the first 8 h, remaining almost constant until 10 days, after which it decreased gradually to 3.3 (Figure 6b). The decline of pH in the iron cathode zone is beneficial to the accumulation of Fe^{2+} and H_2O_2,[14] which enhances MTBE transformation. It is noted that the effluent pH dramatically decreases from 8.5 at the initial 8 h to 6.5 finally (Figure 6b), which means a minimal influence on groundwater chemistry.[53] Since the transformation of MTBE does not show any significant decrease after 20 days of operation, a relatively long longevity can be proposed for the transformation of MTBE in the three-electrode column using an iron cathode.

Implications for Groundwater Remediation. In this study, a new concept of generating Fe^{2+} from an iron cathode is proposed and justified for in situ Pd-catalytic transformation of MTBE in groundwater. Kinetic analysis and experimental results show that the accumulation of Fe^{2+} can be quantitatively related to the cathodic current applied on the iron and the solution pH. In a specially configured three-electrode column using an iron cathode, both the pH and Fe^{2+} accumulation in the Pd vicinity are determined by the current applied on the iron cathode, and MTBE transformation can be sustained at high levels for relatively long periods of time. Fe^{2+}

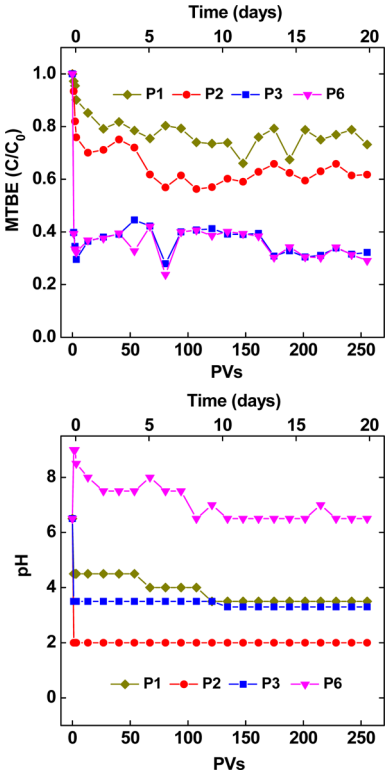

Figure 6. Long-term performance of the three-electrode column using an iron cathode for (a) MTBE transformation and (b) pH variation. P1, P2, P3, and P6 denote different sampling ports (see Figure S2 for details). Operation conditions are based on 10 mg/L initial MTBE concentration, 5 mM Na_2SO_4 and 0.5 mM $CaSO_4$ electrolyte, 2.5 mL/min, and a total current of 80 mA with 50 and 30 mA partitioned in cathodes 1 and 2.

concentration can be exclusively regulated by the current being applied on the iron cathode, providing a manipulable approach to supplying Fe^{2+} for the Pd-based E-Fenton process in iron-defective aquifers. This finding also throws light on the controllable production of Fe^{2+} for conventional E-Fenton processes, i.e., using one iron cathode and one O_2 reduction cathode, and the other processes requiring Fe^{2+} such as Fenton-based processes and in situ persulfate oxidation.

As the main barriers of in situ Fe^{2+} supply and pH adjustments have been removed to some extent and the feasibility of transforming contaminants in real groundwater is demonstrated, the conceptual model applying this improved Pd-based E-Fenton process is illustrated in Figure S12. Since all the reactants (Fe^{2+} and H_2O_2) and reaction conditions (~pH 3) are automatically produced, it is not necessary to add any chemicals during the course of treatment. Moreover, the overall impact on aquifer chemistry would be minimal since the only chemical introduced is the low concentration of Fe^{2+}. The cost of Pd catalyst and electrical energy consumption as well as the influence of groundwater chemistry are the other concerns for the application of this process. Pd catalyst is costly but can be used for a long time. The long-term operation of Pd-catalytic hydrodechlorination in a field test showed that the catalyst activity can be maintained for several years.[54] The fast development of solar panels offers a possibility of decreasing the cost of electric consumption, although problems exist currently.[17] Groundwater chemistry may negatively affect the efficiency by precipitates forming, microorganism growth,

dx.doi.org/10.1021/es401730s | Environ. Sci. Technol. 2013, 47, 7918−7926

bicarbonate buffering, $^{\bullet}OH$ scavenging, Pd foiling, and so on. The localized low pH developed in the reaction zone can alleviate the precipitation of groundwater cations (i.e., Ca^{2+} and Mg^{2+})[55] and inhibit the growth of microorganism on the catalyst surface.[15] Bicarbonate buffering slightly affected pH regulation at concentrations up to 5 mM;[15] $^{\bullet}OH$ scavenging by chloride and bicarbonate was also slight at concentrations less than 10 mM.[14] The in situ generated oxidizing species, H_2O_2 and $^{\bullet}OH$, have the potential to resist the fouling of catalyst by reduced sulfur compounds.[14,15] Anodic evolution of free chlorine in the presence of high concentrations of chloride could be risky due to formation of chlorinated byproducts. The risk can be reduced using Ti/MMO (coated with IrO_2/Ta_2O_5) anode which has much lower overpotential for oxygen evolution than for chlorine evolution.[56,57] In addition, the Fe(II) generated in the reaction zone can effectively deplete free chlorine if produced.[58]

■ ASSOCIATED CONTENT

Supporting Information

Additional information: kinetic model for Fe^{2+} accumulation, Figures S1−S12, and Tables S1 and S2. This material is available free of charge via the Internet at http://pubs.acs.org.

■ AUTHOR INFORMATION

Corresponding Author

*Phone: +86-27-67848629. Fax: +86-27-67848629. E-mail: yuansonghu622@hotmail.com.

Notes

The authors declare no competing financial interest.

■ ACKNOWLEDGMENTS

This work was supported by the Natural Science Foundation of China (NSFC, No. 41172220) and the State Key Laboratory of Biogeology and Environmental Geology, China University of Geosciences (No. GBL11204).

■ REFERENCES

(1) Cooper, W. J.; Cramer, C. J.; Martin, N. H.; Mezyk, S. P.; Shea, K. E. O.; Sommtag, C. V. Free radical mechanisms for the treatment of methyl tert-butyl ether (MTBE) via advanced oxidation/reductive processes in aqueous solutions. *Chem. Rev.* **2009**, *109*, 1302−1345.

(2) Hunkeler, D.; Butler, B. J.; Aravena, R.; Barker, J. F. Monitoring biodegradation of methyl tert-butyl ether (MTBE) using compound-specific carbon isotope analysis. *Environ. Sci. Technol.* **2001**, *35*, 676−681.

(3) Acero, J. L.; Handerlein, S. B.; Schmidt, T. C.; Suter, M. J. F.; Gunten, U. V. MTBE oxidation by conventional ozonation and the combination ozone/hydrogen peroxide: Efficiency of the processes and bromate formation. *Environ. Sci. Technol.* **2001**, *35*, 4252−4259.

(4) USEPA. Monitored natural attenuation of MTBE as a risk management option at leaking underground storage tank sites. EPA/600/R-04/179, 2005.

(5) Garrett, P.; Moreau, M.; Lowry J. D. MTBE as a groundwater contaminant. http://info.ngwa.org/gwol/pdf/860142615.PDF (accessed June 12, 2013).

(6) Cooper, W. J.; Tobien, T.; Nickelsen, M. G.; Adams, J. W.; Shea, K. E. O.; Bartels, D. M.; Wishart, J. F.; Tornatore, P. M.; Newman, K. S.; Gregoire, K. Radiation chemistry of methyl tert-butyl ether in aqueous solution. *Environ. Sci. Technol.* **2004**, *38*, 3994−4001.

(7) Yazaydin, A. O.; Thompson, R. W. Molecular simulation of the adsorption of MTBE in silicalite, mordenite, and zeolite beta. *J. Phys. Chem. B* **2006**, *110*, 14458−14462.

(8) Tsitonaki, A.; Petri, B.; Crimi, M.; Mosbaek, H.; Siegrist, R. L.; Bjerg, P. L. In situ chemical oxidation of contaminated soil and groundwater using persulfate: A review. *Crit. Rev. Environ. Sci. Technol.* **2010**, *40*, 55−91.

(9) Johnson, D, C.; Shamamian, V. A.; Callahan, J. H.; Denes, F. S.; Manolache, S. O.; Dandy, D. S. Treatment of methyl tert-butyl ether contaminated water using a dense medium plasma reactor: A mechanistic and kinetic investigation. *Environ. Sci. Technol.* **2003**, *37*, 4804−4810.

(10) Stefan, M. I.; Mack, J.; Bolton, J. R.; Corporation, C. C. Degradation pathways during the treatment of methyl tert-butyl ether by the UV/H_2O_2 process. *Environ. Sci. Technol.* **2000**, *34*, 650−658.

(11) Wu, T. N. Electrocatalytic oxidation of methyl tert-butyl ether (MTBE) in aqueous solution at a nickel electrode. *Chemosphere* **2007**, *69*, 271−278.

(12) Waul, C.; Arvin, E.; Schmidt, J. E. Modeling the competitive effect of ammonium oxidizers and heterotrophs on the degradation of MTBE in a packed bed reactor. *Water Res.* **2008**, *42*, 3098−3108.

(13) Waul, C.; Arvin, E.; Schmidt, J. E. Model description and kinetic parameter analysis of MTBE biodegradation in a packed bed reactor. *Water Res.* **2008**, *42*, 3122−3134.

(14) Yuan, S. H.; Mao, X. H.; Alshawabkeh, A. N. Efficient degradation of TCE in groundwater using Pd and electro-generated H_2 and O_2: A shift in pathway from hydrodechlorination to oxidation in the presence of ferrous ions. *Environ. Sci. Technol.* **2012**, *46*, 3398−3405.

(15) Yuan, S. H.; Chen, M. J.; Mao, X. H.; Alshawabkeh, A. N. A three-electrode column for Pd-catalytic oxidation of TCE in groundwater with automatic pH-regulation and resistance to reduced sulfur compound foiling. *Water Res.* **2013**, *47*, 269−278.

(16) Mao, X. H.; Ciblak, A.; Amiri, M.; Alshawabkeh, A. N. Redox control for electrochemical dechlorination of trichloroethylene in bicarbonate aqueous media. *Environ. Sci. Technol.* **2011**, *45*, 6517−6523.

(17) Mao, X. H.; Yuan, S. H.; Fallahpour, N.; Ciblak, A.; Howard, J.; Padilla, I.; Loch-Caruso, R.; Alshawabkeh, A. N. Electrochemically induced dual reactive barriers for transformation of TCE and mixture of contaminants in groundwater. *Environ. Sci. Technol.* **2012**, *46*, 12003−12011.

(18) Brillas, E.; Casado, J. Aniline degradation by electro-Fenton and peroxi-coagulation processes using a flow reactor for wastewater treatment. *Chemosphere* **2002**, *47*, 241−248.

(19) Pratap, K.; Lemley, A. T. J. Fenton electrochemical treatment of aqueous atrazine and metolachlor. *J. Agric. Food Chem.* **1998**, *46*, 3285−3291.

(20) Wang, Q.; Lemley, A. T. Kinetic model and optimization of 2,4-D degradation by anodic Fenton treatment. *Environ. Sci. Technol.* **2001**, *35*, 4509−4514.

(21) Brillas, E.; Sires, I.; Oturan, A. Electro-Fenton process and related electrochemical technologies based on Fenton's reaction chemistry. *Chem. Rev.* **2009**, *109*, 6570−6631.

(22) Yuan, S. H.; Fan, Y.; Zhang, Y. C.; Tong, M.; Liao, P. Pd-catalytic in situ generation of H_2O_2 from H_2 and O_2 produced by water electrolysis for the efficient electro-Fenton degradation of rhodamine B. *Environ. Sci. Technol.* **2011**, *45*, 8514−8520.

(23) Burbano, A. A.; Dionysiou, D. D.; Suidan, M. T.; Richardson, T. L. Oxidation kinetics and effect of pH on the degradation of MTBE with Fenton reagent. *Water Res.* **2005**, *39*, 107−118.

(24) Burbano, A. A.; Dionysiou, D. D.; Suidan, M. T. Effect of oxidant-to-substrate ratios on the degradation of MTBE with Fenton reagent. *Water Res.* **2008**, *42*, 3225−3239.

(25) Kong, L. J.; Lemley, A. T. Kinetic modeling of 2,4-dichlorophenoxyacetic acid (2,4-D) degradation in soil slurry by anodic Fenton treatment. *J. Agric. Food Chem.* **2006**, *54*, 3941−3950.

(26) Joo, S. H.; Feitz, A. J.; Sedlak, D. L.; Waite, T. D. Quantification of the oxidizing capacity of nanoparticulate zero-valent iron. *Environ. Sci. Technol.* **2005**, *39*, 1263−1268.

(27) Navalon, S.; Alvaro, M.; Garcia, H. Heterogeneous Fenton catalysts based on clays, silicas and zeolites. *Appl. Catal., B* **2010**, *99*, 1−26.

(28) Kong, L. R.; Lu, X. F.; Bian, X. J.; Zhang, W. J.; Wang, C. Constructing carbon-coated Fe_3O_4 microspheres as antiacid and magnetic support for palladium nanoparticles for catalytic applications. *ACS Appl. Mater. Interfaces* **2011**, *3*, 35−42.
(29) He, F.; Zhao, D. Y. Hydrodechlorination of trichloroethene using stabilized Fe-Pd nanoparticles: Reaction mechanism and effects of stabilizers, catalysts and reaction conditions. *Appl. Catal., B* **2008**, *84*, 533−540.
(30) Luo, H. P.; Jin, S.; Fallgren, P. H.; Colberg, P. J. S.; Johnson, P. A. Prevention of iron passivation and enhancement of nitrate reduction by electron supplementation. *Chem. Eng. J.* **2010**, *160*, 185−189.
(31) Henderson, A. D.; Demond, A. H. Long-term performance of zero-valent iron permeable reactive barriers: A critical review. *Environ. Eng. Sci.* **2007**, *24*, 401−423.
(32) Alonso, F.; Beletskaya, I. P.; Yus, M. Metal-mediated reductive hydrodehalogenation of organic halides. *Chem. Rev.* **2002**, *102*, 4009−4091.
(33) Ai, Z. H.; Mei, T.; Liu, J.; L, J. P.; Jia, F. L.; Zhang, L. Z.; Qiu, J. R. $Fe@Fe_2O_3$ core-shell nanowires as an iron reagent. 3. Their combination with CNTs as an effective oxygen-fed gas diffusion electrode in a neutral electro-Fenton system. *J. Phys. Chem. C* **2007**, *111*, 14799−14803.
(34) Kim, S.; Kim, J.; Moon, I. Parameter-based model for the forecasting of pipe corrosion in refinery plants. *Ind. Eng. Chem. Res.* **2011**, *50*, 12626−12629.
(35) Sudrabin, L. P.; Marks, H. C. Cathodic protection of steel in contact with water. *Ind. Eng. Chem.* **1952**, *44*, 1786−1791.
(36) Pedeferri, P. Cathodic protection and cathodic prevention. *Constr. Build. Mater.* **1996**, *10*, 391−402.
(37) Metwally, I. A.; Al-Mandhari, H. M.; Nadir, A. G. Factors affecting cathodic-protection interference. *Eng. Anal. Bound. Elem.* **2007**, *31*, 485−493.
(38) Fallgren, P. H. Use of advanced oxidation and aerobic degradation for remediation of various hydrocarbon contaminates. http://www.osti.gov/bridge/product.biblio.jsp? osti_id=993812 (accessed June 12, 2013).
(39) Guillard, C.; Charton, N.; Pichat, P. Degradation mechanism of t-butyl methyl ether (MTBE) in atmospheric droplets. *Chemosphere* **2003**, *53*, 469−477.
(40) Eisenberg, G. Colorimetric determination of hydrogen peroxide. *Ind. Eng. Chem. Anal. Ed.* **1943**, *15*, 327−328.
(41) Tai, C.; Peng, J. F.; Liu, J. F.; Jiang, G. B.; Zou, H. Determination of hydroxyl radicals in advanced oxidation processes with dimethyl sulfoxide trapping and liquid chromatography. *Anal. Chim. Acta* **2004**, *527*, 73−80.
(42) Komadel, P.; Stucki, J. W. Quantitative assay of minerals for iron(II) and iron(III) using 1,10-phenanthroline. III. A rapid photochemical method. *Clays Clay Miner.* **1988**, *36*, 379−381.
(43) Munakata, N.; Reinhard, M. Palladium-catalyzed aqueous hydrodechlorination in column reactors: Modeling of deactivation kinetics with sulfite and comparison of regenerants. *Appl. Catal., B* **2007**, *75*, 1−10.
(44) Lowry, G. V.; Reinhard, M. Pd-Catalyzed TCE dechlorination in groundwater: solute effects, biological control, and oxidative catalyst regeneration. *Environ. Sci. Technol.* **2010**, *34*, 3217−3223.
(45) Arnold, S. M.; Hickey, W. J.; Harris, R. F. Degradation of atrazine by Fenton's reagent: Condition optimization and product quantification. *Environ. Sci. Technol.* **1995**, *29*, 2083−2089.
(46) Buxton, G. V.; Greenstock, C. L.; Helman, W. P.; Ross, A. B. Critical review of rate constants for reactions of hydrated electrons, hydrogen atoms and hydroxyl radicals ($\bullet OH/\bullet O^-$) in aqueous solution. *J. Phys. Chem. Ref. Data* **1988**, *17*, 513−886.
(47) Hong, S.; Zhang, H.; Duttweiler, C. M.; Lemley, A. T. Degradation of methyl tertiary-butyl ether (MTBE) by anodic Fenton treatment. *J. Hazard. Mater.* **2007**, *144*, 29−40.
(48) Uhlig, H. H.; Revie, R. W. *Corrosion and Corrosion Control*; John Wiley: New York, 1985.
(49) Stumm, W.; Lee, F. G. Oxygenation of ferrous iron. *Ind. Eng.Chem.* **1961**, *53*, 143−146.
(50) Bergendahl, J. A.; Thies, T. P. Fenton's oxidation of MTBE with zero-valent iron. *Water Res.* **2004**, *38*, 327−334.
(51) Kiwi, J.; Lopez, A.; Nadtochenko, V. Mechanism and kinetics of the OH-radical intervention during Fenton oxidation in the presence of a significant amount of radical scavenger (Cl^-). *Environ. Sci. Technol.* **2000**, *34*, 2162−2168.
(52) Kang, S. H.; Choi, W. Y. Oxidative degradation of organic compounds using zero-valent iron in the presence of natural organic matter serving as an electron shuttle. *Environ. Sci. Technol.* **2009**, *43*, 878−883.
(53) Fontes, D. E.; Mills, A. L.; Hornberger, G. M.; Herman, J. S. Physical and chemical factors influencing transport of microorganisms through porous-media. *Appl. Environ. Microbiol.* **1991**, *57*, 2473−2481.
(54) Davie, M. G.; Cheng, H. F.; Hopkins, G. D.; LeBron, C. A.; Reinhard, M. Implementing heterogeneous catalytic dechlorination technology for remediating TCE-contaminated groundwater. *Environ. Sci. Technol.* **2008**, *42*, 8908−8915.
(55) Lowry, G. V.; Reinhard, M. Pd-catalyzed TCE dechlorination in water: Effects of $[H_2](aq)$ and H_2-utilizing competitive solutes on the TCE dechlorination rate and product distribution. *Environ. Sci. Technol.* **2001**, *35*, 696−702.
(56) Pikaar, I.; Rozendal, R. A.; Yuan, Z.; Keller, J.; Rabaey, K. Electrochemical sulfide oxidation from domestic wastewater using mixed metal-coated titanium electrodes. *Water Res.* **2011**, *45*, 5381−5388.
(57) Petersen, M. A.; Sale, T. C.; Reardon, K. F. Electrolytic trichloroethene degradation using mixed metal oxide coated titanium mesh electrodes. *Chemosphere* **2007**, *67*, 1573−1581.
(58) Riggle, J. W.; Tepe, J. B. Absorption of chlorine in ferrous sulfate solutions. *Ind. Eng. Chem.* **1950**, *42*, 1036−1041.